Magnetism of the spin-1 tetramer compound $A_2Ni_2Mo_3O_{12}$ (A = Rb or K)

Masashi Hase,[1,*] Akira Matsuo,[2] Koichi Kindo,[2] and Masashige Matsumoto[3]

[1]*Research Center for Advanced Measurement and Characterization, National Institute for Materials Science (NIMS), 1-2-1 Sengen, Tsukuba-shi, Ibaraki 305-0047, Japan*

[2]*The Institute for Solid State Physics (ISSP), The University of Tokyo, 5-1-5 Kashiwanoha, Kashiwa-shi, Chiba 277-8581, Japan*

[3]*Department of Physics, Shizuoka University, 836 Ohya, Suruga-ku, Shizuoka-shi, Shizuoka 422-8529, Japan*

(Received 11 October 2017; revised manuscript received 30 November 2017; published 19 December 2017)

We measured the temperature dependence of the magnetic susceptibility $\chi(T)$ and the specific heat $C(T)$ and the magnetic-field dependence of the magnetization $M(H)$ of $A_2Ni_2Mo_3O_{12}$ (A = Rb or K) powder. We consider that the probable spin model is an interacting spin-1 antiferromagnetic tetramer model. We evaluated values of the intratetramer interactions as $J_1 = 9$ K and $J_2 = 18$ K, and the effective intertetramer interaction as $J_{\rm eff} = 4$ K for $Rb_2Ni_2Mo_3O_{12}$. The susceptibility and magnetization at 1.3 K of $K_2Ni_2Mo_3O_{12}$ are very close to those of $Rb_2Ni_2Mo_3O_{12}$. We observed a phase transition to a magnetically ordered state in $C(T)/T$ in magnetic fields above 3 T. The transition temperature increases with magnetic field. Probably, the ordered state appears around 1.8 K even in 0 T. The ordered state in 0 T, however, is not stable enough like an order in the vicinity of a quantum critical point. Longitudinal-mode magnetic excitations may be observable in single crystalline $A_2Ni_2Mo_3O_{12}$ (A = Rb or K).

DOI: 10.1103/PhysRevB.96.214424

I. INTRODUCTION

Two types of magnetic excitations exist in a magnetically ordered state. They are gapless transverse-mode (Nambu-Goldstone mode) [1] and gapped longitudinal-mode (amplitude Higgs mode) [2–6] excitations corresponding to fluctuations in directions perpendicular and parallel to ordered moments, respectively. The transverse-mode (T-mode) excitations are well known as spin wave excitations. Investigations of the longitudinal-mode (L-mode) excitations are now in progress. The L-mode excitation has weak intensity and spontaneously decays into a pair of T-mode excitations [7,8]. However, it can be well-defined in the ordered state in the vicinity of the quantum critical point [9]. In interacting antiferromagnetic (AF) spin-$\frac{1}{2}$ dimer compounds $TlCuCl_3$ and $KCuCl_3$, the ground state (GS) is a spin-singlet state at atmospheric pressure and zero magnetic field. The L-mode excitations were actually observed in a pressure-induced magnetically ordered state of $TlCuCl_3$ and $KCuCl_3$ by inelastic neutron scattering (INS) experiments [10–12] and Raman scattering experiments [13,14], respectively, and in a magnetic-field-induced ordered state of $TlCuCl_3$ by Raman scattering experiments [15].

According to results of theoretical investigations, the L-mode excitations may be observed in an antiferromagnetically ordered state appearing on cooling at atmospheric pressure and zero magnetic field in interacting spin-cluster compounds [16]. A shrinkage of ordered magnetic moments by quantum fluctuations leads to a large intensity of the L-mode excitations. If the GS of the corresponding isolated spin cluster is a spin-singlet state, the shrinkage of ordered moments can be expected in an ordered state of the interacting spin-cluster compounds. In interacting spin clusters, the ordered state can appear under the condition that the value of Δ is comparable to or less than that of an effective intercluster interaction [16]. Here Δ is the energy difference (spin gap) between the singlet GS and lowest triplet states in the isolated cluster. The effective intercluster interaction is given by the sum of the products of the absolute value of each intercluster interaction ($|J_{{\rm int},i}|$) and the corresponding number of interactions per spin (z_i) as $J_{\rm eff} = \sum_i z_i |J_{{\rm int},i}|$. The effective intercluster interaction is usually smaller than dominant intracluster interactions. Therefore it is advantageous to the appearance of the ordered state that Δ is smaller than dominant intracluster interactions. In the AF spin dimer given by $JS_1 \cdot S_2$, the value of Δ/J is 1 irrespective of the spin value. It is rare that spin dimer compounds show a magnetically ordered state at atmospheric pressure and zero magnetic field. Examples are NH_4CuCl_3 (spin $\frac{1}{2}$) [17,18] and $CrVMoO_7$ (spin $\frac{3}{2}$) [19].

In a spin tetramer expressed by the following Hamiltonian with $J_1 > 0$ or $J_2 > 0$, the GS is a spin-singlet state [20]. The Hamiltonian is

$$\mathcal{H} = J_1 S_2 \cdot S_3 + J_2(S_1 \cdot S_2 + S_3 \cdot S_4). \quad (1)$$

Δ/J_1 can be sufficiently small [21–24]. Interacting spin tetramers are advantageous to the appearance of the ordered state. Several spin tetramer compounds having a magnetically ordered state have been reported. Table I shows values of J_1, J_2, Δ, and $T_{\rm N}$ of the spin tetramer compounds. Magnetic excitations in $Cu_2^{114}Cd^{11}B_2O_6$ were studied by INS experiments on its powder [23]. The results suggest the existence of the L-mode excitations. It is important to investigate the L-mode excitations in the known spin tetramer compounds using single crystals. It is also important to find more spin tetramer compounds having an antiferromagnetically ordered state. We can expect spin-1 tetramers in $A_2Ni_2Mo_3O_{12}$ (A = Rb or K) from its crystal structure [27,28]. We report magnetism of these compounds.

II. EXPECTED SPIN SYSTEM

The two compounds $A_2Ni_2Mo_3O_{12}$ (A = Rb or K) are isostructural. The space group is $P2_1/c$ (No. 14). The lattice constants are $a = 6.996$, $b = 9.186$, $c = 19.895$ Å, and

*HASE.Masashi@nims.go.jp

TABLE I. Values of the exchange interaction parameters, the spin gap of the isolated tetramers, and the AF transition temperature in the spin tetramer compounds. In $Cu_2Fe_2Ge_4O_{13}$, Cu^{2+} and Fe^{3+} ions have spins 1/2 and 5/2, respectively. The spin tetramers Fe-Cu-Cu-Fe are formed. In $Rb_2Ni_2Mo_3O_{12}$, T_N in 0 T was estimated from the extrapolation of $T_N(H)$.

	spin	J_1 (K)	J_2 (K)	Δ (K)	T_N	Ref.
$Cu_2CdB_2O_6$	$\frac{1}{2}$	317	−162	19	9.8	[23]
$CuInVO_5$	$\frac{1}{2}$	240	−142	17	2.7	[24]
$SeCuO_3$	$\frac{1}{2}$	225	160	84	8	[25]
$Cu_2Fe_2Ge_4O_{13}$	$\frac{1}{2}$, $\frac{5}{2}$	255	26.7	1.3	39	[16,26]
$Rb_2Ni_2Mo_3O_{12}$	1	9	18	12	1.8(2)	this work

$\beta = 108.71°$ in $Rb_2Ni_2Mo_3O_{12}$ [27]. They are $a = 6.952$, $b = 8.910$, $c = 19.733$ Å, and $\beta = 108.06°$ in $K_2Ni_2Mo_3O_{12}$ [28]. The Ni^{2+} ions ($3d^8$) have localized spin-1. The positions of the Ni ions and the O ions connected to the Ni ions are shown schematically in Fig. 1(a). Two crystallographic Ni sites (Ni1 and Ni2) exist. Red and blue bars indicate two types of short Ni-Ni pairs. We show the Ni-Ni distances and Ni-O-Ni angles in Table II. If dominant exchange interactions exist in the Ni-Ni pairs, spin tetramers given by Eq. (1) are formed. The other Ni-Ni lengths are 4.999 (4.961) Å or greater in $Rb_2Ni_2Mo_3O_{12}$ ($K_2Ni_2Mo_3O_{12}$). Crystal structures depend on A and M in compounds expressed as $A_2M_2Mo_3O_{12}$ (A = alkali metal and $M = 3d$ metal). There are several types of spin systems. For example, the spin system is a frustrated spin-$\frac{1}{2}$ chain in $A_2Cu_2Mo_3O_{12}$ (A = Rb or Cs) [29,30].

Figure 1(b) shows NiO_6 octahedra. Table III shows Ni-O lengths and O-Ni-O angles in the octahedra. The $Ni1O_6$ and $Ni2O_6$ octahedra are similar to each other. The symmetries of crystal fields affecting the Ni^{2+} ions are not so far from cubic. We expect that the single-ion anisotropy is small.

III. EXPERIMENTAL AND CALCULATION METHODS

Crystalline $A_2Ni_2Mo_3O_{12}$ (A = Rb or K) powder was synthesized by a solid-state reaction. Starting materials are Rb_2CO_3 (purity 99 %), K_2CO_3 (purity 99.9 %), NiO (purity 99.97 %), and MoO_3 (purity 99.99 %) powder. Stoichiometric mixtures of powder were sintered at 853 and 923 K in air for 150 h with intermediate grindings for the Rb and K compounds, respectively. We measured x-ray powder diffraction patterns at room temperature using an x-ray diffractometer (RINT-TTR III; Rigaku). We confirmed that each sample was a nearly single phase of $A_2Ni_2Mo_3O_{12}$ (A = Rb or K).

We measured the magnetization in magnetic fields of up to 5 T using a superconducting quantum interference device magnetometer magnetic property measurement system (Quantum Design). High-field magnetization measurements were conducted using an induction method with a multilayer pulsed field magnet installed at the Institute for Solid State Physics (ISSP), the University of Tokyo. We used a physical property measurement system (Quantum Design) for the specific heat measurements. We measured the specific heat in magnetic fields of not only $Rb_2Ni_2Mo_3O_{12}$ but also $CuInVO_5$ and $CrVMoO_7$ for comparison.

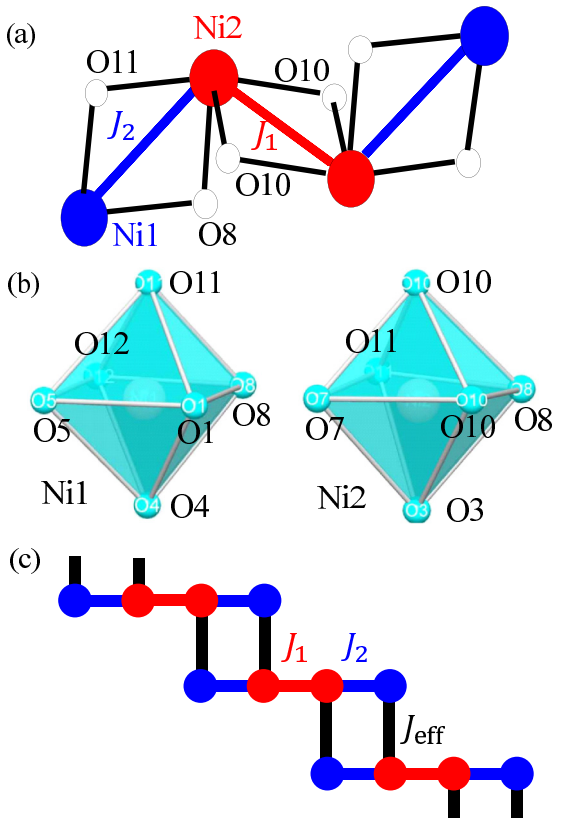

FIG. 1. (a) Schematic drawing of positions of Ni^{2+} ions having spin-1 and O^{2-} ions connected to Ni^{2+} ions in $A_2Ni_2Mo_3O_{12}$ (A = Rb or K) [27,28]. Blue, red, and white circles indicate Ni1, Ni2, and O sites, respectively. Red and blue bars indicate two types of short Ni-Ni pairs. We define J_1 and J_2 as the exchange interaction parameters for the Ni2-Ni2 and Ni1-Ni2 pairs, respectively. The J_1 and J_2 interactions form a spin-1 tetramer. (b) NiO_6 octahedra of Ni1 (left) and Ni2 (right). (c) Interacting spin-1 tetramer model used to calculate magnetization using a mean-field theory based on the tetramer unit (tetramer mean-field theory). We adopted the interaction in the third shortest Ni-Ni pair (4.999 Å) as the effective intertetramer interaction (J_{eff}).

We obtained eigenenergies of isolated spin-1 tetramers using an exact diagonalization method. We calculated the temperature dependence of the magnetic susceptibility $\chi(T)$ and the specific heat $C(T)$, and the magnetic-field dependence of the magnetization $M(H)$ using the eigenenergies.

We calculated $M(H)$ for the model shown in Fig. 1(c) using a mean-field theory based on the tetramer unit (tetramer

TABLE II. Ni-Ni lengths and Ni-O-Ni angles in the two types of short Ni-Ni pairs in $A_2Ni_2Mo_3O_{12}$ (A = Rb or K).

		Rb		K	
		Ni-Ni length (Å)	Ni-O-Ni angle (deg.)	Ni-Ni length (Å)	Ni-O-Ni angle (deg.)
J_1	Ni2-Ni2	3.174	97.48 (O10)	3.128	96.24 (O10)
J_2	Ni1-Ni2	3.081	96.31 (O8)	3.089	97.89 (O8)
			93.64 (O11)		93.96 (O11)

TABLE III. Ni-O lengths and O-Ni-O angles in NiO octahedra in $Rb_2Ni_2Mo_3O_{12}$. The deviation is defined as the difference between each Ni-O length and the average Ni-O length [$L_{ave,i}(i = 1,2)$] divided by $L_{ave,i}$. The values of $L_{ave,i}$ are 2.080 and 2.062 Å for Ni1-O and Ni2-O, respectively. The maximum deviation in the Ni-O lengths from the average is 0.045. The minimum and maximum O-Ni-O angles are 81.88° and 101.18°, respectively.

	Å	deviation		Å	deviation
Ni1-O4	2.024	0.027	Ni2-O7	2.023	0.019
O1	2.035	0.022	O3	2.032	0.014
O5	2.058	0.011	O8	2.044	0.009
O8	2.092	0.006	O11	2.050	0.006
O12	2.098	0.009	O10(2)	2.077	0.007
O11	2.174	0.045	O10(4)	2.145	0.040
	degrees			degrees	
O11-Ni1-O1	90.58		O10(4)-Ni2-O7	84.43	
O5	92.02		O8	88.76	
O8	82.48		O10(2)	82.52	
O12	81.88		O11	83.03	
O4-Ni1-O1	92.04		O3-Ni2-O7	95.17	
O5	93.38		O8	91.67	
O8	91.92		O10(2)	101.18	
O12	95.31		O11	93.33	
O12-Ni1-O5	88.43		O10(2)-Ni2-O7	92.56	
O8	86.99		O8	85.83	
O1-Ni1-O5	93.49		O11-Ni2-O7	93.09	
O8	90.42		O8	86.78	
O11-Ni1-O4	173.84		O10(4)-Ni2-O3	176.30	
O12-Ni1-O1	172.28		O10(2)-Ni2-O11	163.89	
O8-Ni1-O5	173.29		O8-Ni2-O7	173.16	

mean-field theory). Finite magnetic moments were initially assumed on the Ni sites in the tetramer. The mean-field Hamiltonian was then expressed by a 81×81 matrix form under consideration of the external magnetic field and the molecular field from neighboring tetramers. The eigenstates of the mean-field Hamiltonian were used to calculate the expectation value of the ordered moments on the Ni sites. We continued this procedure until the values of the magnetic moments converged. We finally obtained a self-consistently determined solution for $M(H)$.

IV. RESULTS AND DISCUSSION

Figure 2 shows the temperature T dependence of the magnetic susceptibility $\chi(T)$ of $A_2Ni_2Mo_3O_{12}$ (A = Rb or K) in a magnetic field of $H = 0.01$ T. The susceptibilities of the two compounds are very close to each other. A broad maximum can be seen around 16 K, indicating a low-dimensional AF spin system. The susceptibility decreases rapidly at low T. However, $\chi(T)$ does not seem to approach a small value at 0 K expected for a spin singlet GS with a spin gap [31–33]. Figure 3 shows the magnetic field H dependence of the magnetization $M(H)$ of $Rb_2Ni_2Mo_3O_{12}$ at 2 K. The magnetization has the finite slope even around 0 T, indicating that the GS is magnetic. The red circles in the inset of Fig. 4(a) show the specific heat divided by T [$C(T)/T$] of $Rb_2Ni_2Mo_3O_{12}$ in 0 T. A broad maximum can be seen around 5 K, indicating a low-dimensional AF spin system. $C(T)/T$ seems to approach zero at 0 K, indicating no T-linear term. A spin liquid state cannot be expected [34]. We will describe later the results in finite magnetic fields.

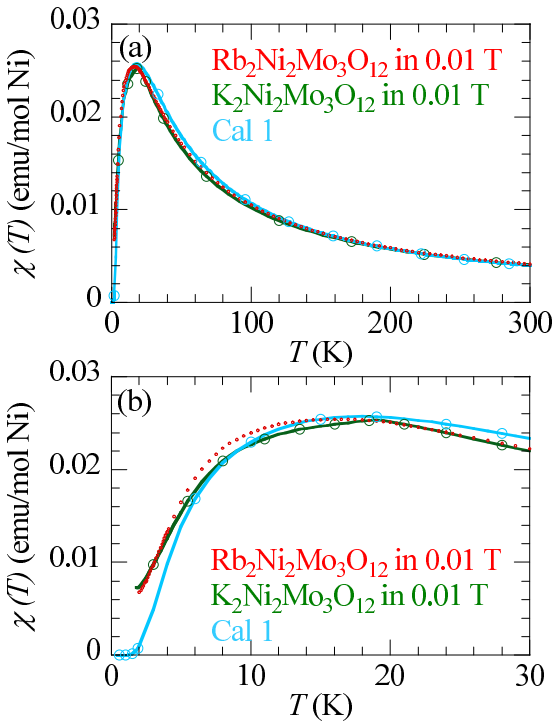

FIG. 2. Temperature T dependence of the magnetic susceptibility $\chi(T)$ of $Rb_2Ni_2Mo_3O_{12}$ (red circles) and $K_2Ni_2Mo_3O_{12}$ (green line) in a magnetic field of $H = 0.01$ T below 300 K (a) and 30 K (b). The light-blue line indicates $\chi(T)$ calculated for the isolated spin-1 tetramer with $J_1 = 9$ K and $J_2 = 18$ K.

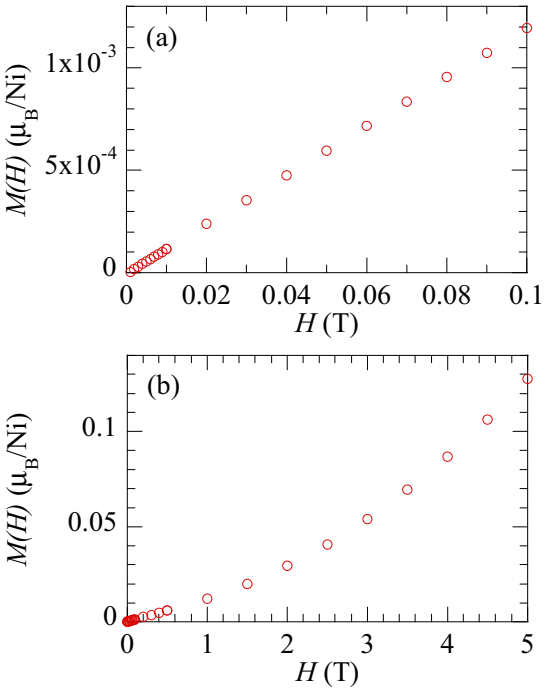

FIG. 3. Magnetic field H dependence of the magnetization $M(H)$ of $Rb_2Ni_2Mo_3O_{12}$ at 2 K below 0.1 T (a) and 5 T (b).

The red lines in Fig. 5 show $M(H)$ of $Rb_2Ni_2Mo_3O_{12}$. The magnetization at 1.3 K increases monotonically and is saturated around 45 T. The g value was evaluated to be 2.24 from the saturated magnetization. The saturation is also seen at 4.2 K and is smeared above 10 K. As shown in the inset of Fig. 5, the magnetizations of the two compounds at 1.3 K are very close to each other.

We compared experimental $\chi(T)$ and $M(H)$ at 1.3 K with those calculated for the isolated spin-1 tetramer model expressed in Eq. (1). The experimental results are close to the calculated ones with $J_1 = 9$ K and $J_2 = 18$ K indicated by the light-blue lines in Figs. 2 and 5. The light-blue line in the inset of Fig. 4(a) indicates $C(T)/T$ calculated for the same model. We cannot evaluate precisely the magnetic specific heat of $Rb_2Ni_2Mo_3O_{12}$. Although the red circles in the inset of Fig. 4(a) show the total $C(T)/T$ including lattice specific heat, the experimental and calculated results are similar to each other.

The experimental $M(H)$ at 1.3 K increases monotonically up to the saturation, whereas the calculated $M(H)$ at 1.3 K shows quantum magnetization plateaus. According to the results in $CuInVO_5$ [24] and $CrVMoO_7$ [19], the discrepancy between the experimental and calculated $M(H)$ is probably caused by intertetramer interactions. It is difficult, however, to determine which intertetramer interactions are effective. We adopted the interaction in the third shortest Ni-Ni pair (4.999 Å) as the effective intertetramer interaction ($J_{\rm eff}$). Figure 1(c) shows schematically the interacting spin-1 tetramer model.

The blue lines in Fig. 5 indicate $M(H)$ calculated for the interacting spin-1 tetramer model using the tetramer mean-field theory. The values of the exchange interactions are $J_1 = 9$ K, $J_2 = 18$ K, and $J_{\rm eff} = 4$ K. The experimental and calculated $M(H)$ at 1.3 K are in agreement with each other.

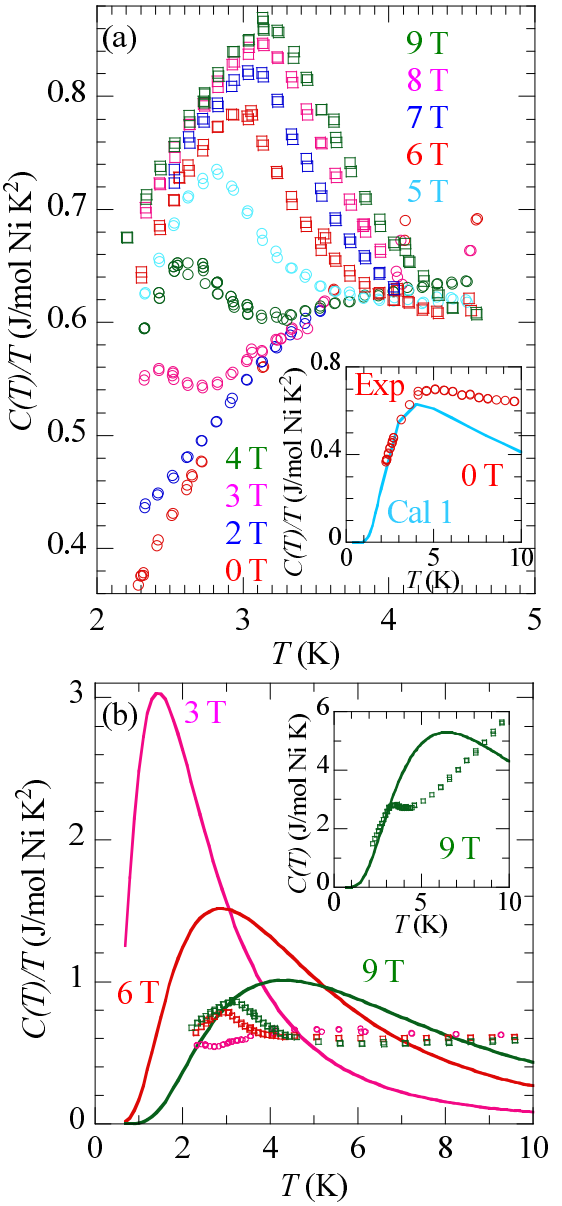

FIG. 4. (a) Temperature T dependence of the specific heat divided by T $[C(T)/T]$ of $Rb_2Ni_2Mo_3O_{12}$ in various magnetic fields. The inset shows $C(T)/T$ in zero magnetic field below 10 K. The light-blue line indicates $C(T)/T$ calculated for the isolated spin-1 tetramer with $J_1 = 9$ K and $J_2 = 18$ K. (b) $C(T)/T$ of $Rb_2Ni_2Mo_3O_{12}$ in 3, 6, and 9 T indicated by pink circles, red squares, and green squares, respectively. Lines indicate calculated Schottky specific heat of $g = 2$. The inset shows $C(T)$ of $Rb_2Ni_2Mo_3O_{12}$ (squares) and the Schottky specific heat (line) in 9 T.

The calculated $M(H)$, however, is larger than the experimental $M(H)$ in high fields at 10 K and higher Ts. As J_1 or J_2 increases, the calculated $M(H)$ at high T approaches the experimental $M(H)$, whereas the discrepancy between the experimental and calculated results of $M(H)$ at low T and $\chi(T)$ becomes apparent. We also calculated $M(H)$ for the interacting spin-1 tetramer model including the D term of the single-ion anisotropy. Here, the Hamiltonian of the single-ion anisotropy is expressed as $\mathcal{H}_s = D(S^z)^2$. The calculated $M(H)$

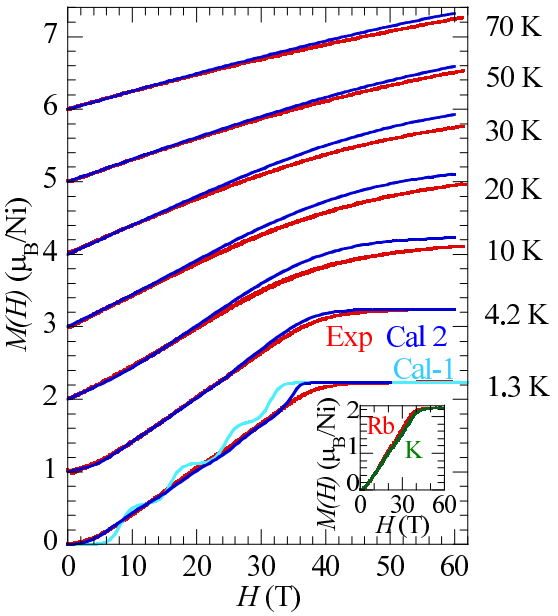

FIG. 5. Magnetic field H dependence of the magnetization $M(H)$ of $Rb_2Ni_2Mo_3O_{12}$ (red lines) at various temperatures. Light-blue and blue lines indicate $M(H)$ calculated for the isolated spin-1 tetramer model labeled by "cal 1" and for the interacting spin-1 tetramer model in Fig. 1(c) labeled by "cal 2," respectively. The values of the parameters are $J_1 = 9$ K, $J_2 = 18$ K, $J_{\rm eff} = 4$ K, and $g = 2.44$. Vertical positions are shifted by 1 μ_B/Ni per line. The inset shows $M(H)$ at 1.3 K of $Rb_2Ni_2Mo_3O_{12}$ (red) and $K_2Ni_2Mo_3O_{12}$ (green).

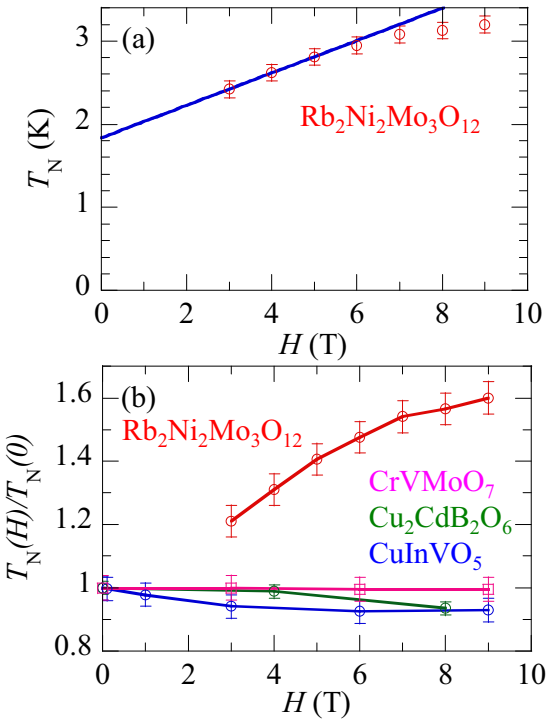

FIG. 6. (a) Magnetic field H dependence of the AF transition temperature $T_N(H)$ of $Rb_2Ni_2Mo_3O_{12}$. The line is a guide to eyes. (b) Magnetic field H dependence of $T_N(H)/T_N(0)$ of the spin tetramer compounds $Rb_2Ni_2Mo_3O_{12}$, $Cu_2CdB_2O_6$, and $CuInVO_5$. We used 2 K as $T_N(0)$ of $Rb_2Ni_2Mo_3O_{12}$ [the upper limit of estimated $T_N(0)$]. The results of the spin-3/2 dimer compound $CrVMoO_7$ are also shown as reference.

depends on the D value strongly and weakly at low and high T, respectively. The present discrepancy between the experimental and calculated $M(H)$ could not be reduced by the introduction of the D term.

We can see 0, $\frac{1}{4}$, $\frac{1}{2}$, and $\frac{3}{4}$ magnetization plateaus in the calculated line of the isolated spin-1 tetramer model at 1.3 K. The $\frac{1}{4}$, $\frac{1}{2}$, and $\frac{3}{4}$ magnetization-plateau phases are polarized paramagnetic phases in which $S_z^{\rm T} = -1, -2,$ and -3, respectively. Here, $S_z^{\rm T}$ represents the z value of the total spin of the four $S = 1$ spins. In interacting spin tetramers, an ordered phase can appear in a magnetic-field range where $M(H)$ increases. As described later, the specific-heat results indicate a magnetically ordered phase at low T in $Rb_2Ni_2Mo_3O_{12}$. No magnetization plateau in experimental lines indicates a single magnetically ordered phase is formed until the saturation of the magnetization [19].

Superexchange interactions are probably ferromagnetic in the two types of short Ni-Ni pairs because of the Ni-O-Ni angles. Antiferromagnetic direct exchange interactions are also expected because of the short Ni-Ni lengths. We infer that the summation of the ferromagnetic superexchange interactions and AF direct exchange interaction generates the small AF J_1 and J_2 interactions.

Figure 4(a) shows $C(T)/T$ of $Rb_2Ni_2Mo_3O_{12}$ in various magnetic fields. We can see a peak above 3 T. The peak is not caused by isolated Ni^{2+} spins of impurities showing the Schottky specific heat. Figure 4(b) shows $C(T)/T$ of $Rb_2Ni_2Mo_3O_{12}$ and that of the Schottky specific heat of $g = 2$. The Schottky specific heat has a stronger H dependence than $Rb_2Ni_2Mo_3O_{12}$. The H dependence of the Schottky specific heat is stronger when g is larger. The inset of Fig. 4(b) shows $C(T)$ in 9 T of $Rb_2Ni_2Mo_3O_{12}$ and the Schottky specific heat of $g = 2$. The peak positions are different from each other. The difference is larger when g is larger. Consequently, the peaks in $C(T)/T$ of $Rb_2Ni_2Mo_3O_{12}$ indicate a phase transition to a magnetically ordered state.

Figure 6(a) shows the H dependence of the peak temperature $T_N(H)$ in $C(T)/T$ of $Rb_2Ni_2Mo_3O_{12}$. The peak temperature increases with H. As suggested by the blue line, we infer that the ordered state appears around 1.8 K even in 0 T. This inference is consistent with the susceptibility and magnetization results indicating that the GS is magnetic.

Figure 6(b) shows the H dependence of $T_N(H)/T_N(0)$ of the spin tetramer compounds $Rb_2Ni_2Mo_3O_{12}$, $Cu_2CdB_2O_6$ [35], and $CuInVO_5$, and the spin-3/2 dimer compound $CrVMoO_7$. As H is increased, $T_N(H)/T_N(0)$ increases in $Rb_2Ni_2Mo_3O_{12}$, whereas $T_N(H)/T_N(0)$ is almost constant or decreases slightly in the other three compounds. The phase transition temperature increases with H in the spin-tetrahedra system $Cu_2Te_2O_5Br_2$ [36]. Investigations using chemical and hydrostatic pressure suggest the closeness of the system to a quantum critical point [37–40]. In $Rb_2Ni_2Mo_3O_{12}$, we speculate that the order in 0 T is not stable enough like an order in the vicinity of a quantum critical point [10–12] and that the order is stabilized by the application of magnetic fields.

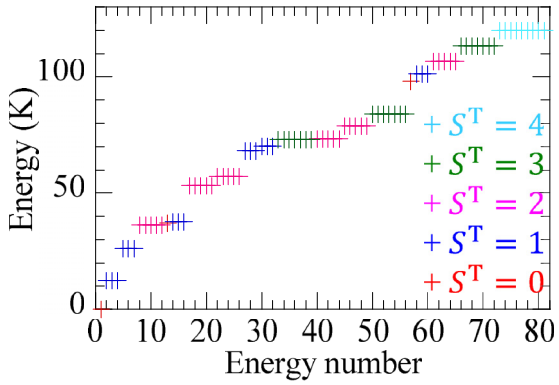

FIG. 7. Eigenenergies measured from the spin-singlet ground state in the isolated spin-1 tetramer with $J_1 = 9$ K and $J_2 = 18$ K.

Figure 7 shows the eigenenergies measured from the spin-singlet GS in the isolated spin-1 tetramer with $J_1 = 9$ K and $J_2 = 18$ K. The spin gap value (12 K) is smaller than the dominant J_2 value and is larger than the $J_{\rm eff}$ value (4 K). We consider that the order in 0 T is not stable enough because of the small $J_{\rm eff}$ value.

In future, we will make single crystals of $A_2Ni_2Mo_3O_{12}$ (A = Rb or K) and evaluate the single-ion anisotropy. We will determine the magnetic structure by neutron diffraction experiments. We will confirm the signs of J_1 and J_2 from the magnetic structure. We will consider which intertetramer interactions are effective to stabilize the magnetic structure. We will calculate $\chi(T)$ and $M(H)$ of a more realistic model using quantum Monte Carlo techniques and reproduce the experimental results.

As described, the order of $Rb_2Ni_2Mo_3O_{12}$ in 0 T may be similar to an order in the vicinity of a quantum critical point. The L-mode magnetic excitations may be observable like in the pressure-induced or magnetic-field-induced magnetically ordered state of the interacting AF spin-$\frac{1}{2}$ dimer compounds $TlCuCl_3$ and $KCuCl_3$ [10–15]. We intend to perform inelastic neutron scattering and Raman scattering experiments to investigate L-mode magnetic excitations. In the weakly ordered spin-$\frac{1}{2}$ chain antiferromagnet Sr_2CuO_3, unusual magnetic excitations were recently observed by ESR experiments [41]. It is reported that the excitations can be attributed to the Nambu-Goldstone mode renormalized due to its interaction with the high-energy L-mode. We also pursue such unusual excitations in $A_2Ni_2Mo_3O_{12}$ (A = Rb or K).

V. CONCLUSION

We measured the temperature T dependence of the magnetic susceptibility $\chi(T)$ and the specific heat $C(T)$ and the magnetic-field H dependence of the magnetization $M(H)$ of $Rb_2Ni_2Mo_3O_{12}$ powder. A broad maximum appears around 16 K in $\chi(T)$. Although $\chi(T)$ decreases rapidly at low T, $\chi(T)$ does not seem to approach a small value at 0 K expected for a spin singlet GS with a spin gap. The low-field magnetization at 2 K has the finite slope even around 0 T. The high-field magnetization at 1.3 K increases monotonically without magnetization plateaus and is saturated around 45 T. The susceptibility and magnetization at 1.3 K of $K_2Ni_2Mo_3O_{12}$ are very close to those of $Rb_2Ni_2Mo_3O_{12}$. The isolated spin-1 antiferromagnetic tetramer model with $J_1 = 9$ K and $J_2 = 18$ K can closely reproduce the experimental susceptibility. We were able to explain the magnetization curves using the interacting spin-1 tetramer model with the effective intertetramer interaction $J_{\rm eff} = 4$ K. In $C(T)/T$, we can see a peak above 3 T, indicating a phase transition to a magnetically ordered state. The transition temperature $T_N(H)$ increases with H. From the H dependence of $T_N(H)$, probably, the ordered state appears around 1.8 K even in 0 T. The ordered state in 0 T, however, is not stable enough like an order in the vicinity of a quantum critical point. Longitudinal-mode magnetic excitations may be observable in single crystalline $A_2Ni_2Mo_3O_{12}$ (A = Rb or K).

ACKNOWLEDGMENTS

This work was financially supported by Japan Society for the Promotion of Science (JSPS) KAKENHI (Grant No. 15K05150) and grants from National Institute for Materials Science (NIMS). M.M. was supported by JSPS KAKENHI (Grant No. 17K05516). The high-field magnetization experiments were conducted under the Visiting Researcher's Program of the Institute for Solid State Physics (ISSP), the University of Tokyo. We are grateful to S. Matsumoto for sample syntheses and x-ray diffraction measurements.

[1] J. Goldstone, A. Salam, and S. Weinberg, Broken symmetries, Phys. Rev. **127**, 965 (1962).
[2] P. W. Higgs, Broken Symmetries and the Masses of Gauge Bosons, Phys. Rev. Lett. **13**, 508 (1964).
[3] S. Sachdev, *Quantum Phase Transitions*, 2nd ed. (Cambridge University Press, Cambridge, 2011).
[4] S. Sachdev and B. Keimer, Quantum criticality, Phys. Today **64**, 29 (2011).
[5] D. Podolsky, A. Auerbach, and D. P. Arovas, Visibility of the amplitude (Higgs) mode in condensed matter, Phys. Rev. B **84**, 174522 (2011).
[6] D. Pekker and C. M. Varma, Amplitude/Higgs modes in condensed matter physics, Annu. Rev. Condens. Matter Phys. **6**, 269 (2015).
[7] Y. Kulik and O. P. Sushkov, Width of the longitudinal magnon in the vicinity of the O(3) quantum critical point, Phys. Rev. B **84**, 134418 (2011).
[8] M. E. Zhitomirsky and A. L. Chernyshev, Colloquium: Spontaneous magnon decays, Rev. Mod. Phys. **85**, 219 (2013).
[9] I. Affleck and G. Wellman, Longitudinal modes in quasi-one-dimensional antiferromagnets, Phys. Rev. B **46**, 8934 (1992).

[10] Ch. Rüegg, B. Normand, M. Matsumoto, A. Furrer, D. F. McMorrow, K. W. Krämer, H.-U. Güdel, S. N. Gvasaliya, H. Mutka, and M. Boehm, Quantum Magnets under Pressure: Controlling Elementary Excitations in $TlCuCl_3$, Phys. Rev. Lett. **100**, 205701 (2008).

[11] P. Merchant, B. Normand, K. W. Krämer, M. Boehm, D. F. McMorrow, and Ch. Rüegg, Quantum and classical criticality in a dimerized quantum antiferromagnet, Nat. Phys. **10**, 373 (2014).

[12] M. Matsumoto, B. Normand, T. M. Rice, and M. Sigrist, Field- and pressure-induced magnetic quantum phase transitions in $TlCuCl_3$, Phys. Rev. B **69**, 054423 (2004).

[13] H. Kuroe, N. Takami, N. Niwa, T. Sekine, M. Matsumoto, F. Yamada, H. Tanaka, and K. Takemura, Longitudinal magnetic excitation in $KCuCl_3$ studied by Raman scattering under hydrostatic pressures, J. Phys.: Conf. Ser. **400**, 032042 (2012).

[14] M. Matsumoto, H. Kuroe, A. Oosawa, and T. Sekine, One-magnon Raman scattering as a probe of longitudinal excitation mode in spin dimer systems, J. Phys. Soc. Jpn. **77**, 033702 (2008).

[15] H. Kuroe, K. Kusakabe, A. Oosawa, T. Sekine, F. Yamada, H. Tanaka, and M. Matsumoto, Magnetic field-induced one-magnon Raman scattering in the magnon Bose-Einstein condensation phase of $TlCuCl_3$, Phys. Rev. B **77**, 134420 (2008).

[16] M. Matsumoto, H. Kuroe, T. Sekine, and T. Masuda, Transverse and longitudinal excitation modes in interacting multispin systems, J. Phys. Soc. Jpn. **79**, 084703 (2010).

[17] B. Kurniawan, M. Ishikawa, T. Kato, H. Tanaka, K. Takizawa, and T. Goto, Novel three-dimensional magnetic ordering in the quantum spin system NH_4CuCl_3, J. Phys.: Condens. Matter **11**, 9073 (1999).

[18] M. Matsumoto, Theoretical study of magnetic excitation in interacting inequivalent spin dimer system NH_4CuCl_3, J. Phys. Soc. Jpn. **84**, 034701 (2015).

[19] M. Hase, Y. Ebukuro, H. Kuroe, M. Matsumoto, A. Matsuo, K. Kindo, J. R. Hester, T. J. Sato, and H. Yamazaki, Magnetism of the antiferromagnetic spin-$\frac{3}{2}$ dimer compound $CrVMoO_7$ having an antiferromagnetically ordered state, Phys. Rev. B **95**, 144429 (2017).

[20] M. Hase, K. M. S. Etheredge, S.-J. Hwu, K. Hirota, and G. Shirane, Spin-singlet ground state with energy gaps in Cu_2PO_4: Neutron-scattering, magnetic-susceptibility, and ESR measurements, Phys. Rev. B **56**, 3231 (1997); In this reference, the Hamiltonian is defined as $\mathcal{H} = \sum_{i,j} 2J_{ij} S_i \cdot S_j$ instead of $\mathcal{H} = \sum_{i,j} J_{ij} S_i \cdot S_j$ in the present paper.

[21] M. Hase, M. Kohno, H. Kitazawa, O. Suzuki, K. Ozawa, G. Kido, M. Imai, and X. Hu, Coexistence of a nearly spin-singlet state and antiferromagnetic long-range order in quantum spin system $Cu_2CdB_2O_6$, Phys. Rev. B **72**, 172412 (2005).

[22] M. Hase, A. Dönni, V. Yu. Pomjakushin, L. Keller, F. Gozzo, A. Cervellino, and M. Kohno, Magnetic structure of $Cu_2CdB_2O_6$ exhibiting a quantum-mechanical magnetization plateau and classical antiferromagnetic long-range order, Phys. Rev. B **80**, 104405 (2009).

[23] M. Hase, K. Nakajima, S. Ohira-Kawamura, Y. Kawakita, T. Kikuchi, and M. Matsumoto, Magnetic excitations in the spin-$\frac{1}{2}$ tetramer substance $Cu_2^{114}Cd^{11}B_2O_6$ obtained by inelastic neutron scattering experiments, Phys. Rev B **92**, 184412 (2015).

[24] M. Hase, M. Matsumoto. A. Matsuo, and K. Kindo, Magnetism of the antiferromagnetic spin-$\frac{1}{2}$ tetramer compound $CuInVO_5$, Phys. Rev. B **94**, 174421 (2016).

[25] I. Živković, D. M. Djokić, M. Herak, D. Pajić, K. Prša, P. Pattison, D. Dominko, Z. Micković, D. Cinčić, L. Forró, H. Berger, and H. M. Rønnow, Site-selective quantum correlations revealed by magnetic anisotropy in the tetramer system $SeCuO_3$, Phys. Rev. B **86**, 054405 (2012).

[26] T. Masuda, A. Zheludev, B. Grenier, S. Imai, K. Uchinokura, E. Ressouche, and S. Park, Cooperative Ordering of Gapped and Gapless Spin Networks in $Cu_2Fe_2Ge_4O_{13}$, Phys. Rev. Lett. **93**, 077202 (2004).

[27] P. V. Klevtsov, V. G. Kim, R. F. Klevtsova, L. A. Glinskaya, and S. F. Solodovnikov, Kristallografiya **33**, 57 (1988) [Double molybdates $Rb_2Me_2^{2+}(MoO_4)_3$ and crystal structure of $Rb_2Ni_2(MoO_4)_3$, Sov. Phys. Crystallogr. **33**, 30 (1988)].

[28] R. F. Klevtsova and L. A. Glinskaya, Crystal structure of potassium nickel molybdate $K_2Ni_2(MoO_4)_3$, J. Struct. Chem. **23**, 816 (1982).

[29] M. Hase, H. Kuroe, K. Ozawa, O. Suzuki, H. Kitazawa, G. Kido, and T. Sekine, Magnetic properties of $Rb_2Cu_2Mo_3O_{12}$ including a one-dimensional spin-1/2 Heisenberg system with ferromagnetic first-nearest-neighbor and antiferromagnetic second-nearest-neighbor exchange interactions, Phys. Rev. B **70**, 104426 (2004).

[30] M. Hase, K. Ozawa, O. Suzuki, H. Kitazawa, G. Kido, H. Kuroe, and T. Sekine, Magnetism of $A_2Cu_2Mo_3O_{12}$ (A = Rb or Cs): Model compounds of a one-dimensional spin-1/2 Heisenberg system with ferromagnetic first-nearest-neighbor and antiferromagnetic second-nearest-neighbor interactions, J. Appl. Phys. **97**, 10B303 (2005).

[31] M. Hase, I. Terasaki, and K. Uchinokura, Observation of the Spin-Peierls Transition in Linear Cu^{2+} (Spin- $\frac{1}{2}$) Chains in an Inorganic Compound $CuGeO_3$, Phys. Rev. Lett. **70**, 3651 (1993).

[32] M. Hase, I. Terasaki, Y. Sasago, K. Uchinokura, and H. Obara, Effects of Substitution of Zn for Cu in the Spin-Peierls Cuprate, $CuGeO_3$: The Suppression of the Spin-Peierls Transition and the Occurrence of a New Spin-Glass State, Phys. Rev. Lett. **71**, 4059 (1993).

[33] M. Hase, I. Terasaki, K. Uchinokura, M. Tokunaga, N. Miura, and H. Obara, Magnetic phase diagram of the spin-Peierls cuprate $CuGeO_3$, Phys. Rev. B **48**, 9616 (1993).

[34] S. Yamashita, Y. Nakazawa, M. Oguni, Y. Oshima, H. Nojiri, Y. Shimizu, K. Miyagawa, and K. Kanoda, Thermodynamic properties of a spin-$\frac{1}{2}$ spin-liquid state in a κ-type organic salt, Nat. Phys. **4**, 459 (2008).

[35] M. Hase, M. Kohno, H. Kitazawa, O. Suzuki, K. Ozawa, G. Kido, M. Imai, and X. Hu, Magnetism of $Cu_2CdB_2O_6$: Quantum spin system having a nearly singlet state and antiferromagnetic long-range order, J. Appl. Phys. **99**, 08H504 (2006).

[36] P. Lemmens, K.-Y. Choi, E. E. Kaul, C. Geibel, K. Becker, W. Brenig, R. Valenti, C. Gros, M. Johnsson, P. Millet, and F. Mila, Evidence for an Unconventional Magnetic Instability in the Spin-Tetrahedra System $Cu_2Te_2O_5Br_2$, Phys. Rev. Lett. **87**, 227201 (2001).

[37] X. Wang, I. Loa, K. Syassen, P. Lemmens, M. Hanfland, and M. Johnsson, The effect of pressure on the structural properties of

the spin-tetrahedra compound $Cu_2Te_2O_5Br_2$, J. Phys.: Condens. Matter **17**, S807 (2005).

[38] J. Kreitlow, S. Süllow, D. Menzel, J. Schoenes, P. Lemmens, and M. Johnsson, Unusual criticality of $Cu_2Te_2O_5Br_2$ under pressure, J. Magn. Magn. Mater. **290-291**, 959 (2005).

[39] S. J. Crowe, M. R. Lees, D. M. K. Paul, R. I. Bewley, J. Taylor, G. McIntyre, O. Zaharko, and H. Berger, Effect of externally applied pressure on the magnetic behavior of $Cu_2Te_2O_5(Br_xCl_{1-x})_2$, Phys. Rev. B **73**, 144410 (2006).

[40] X. Wang, K. Syassen, M. Johnsson, R. Moessner, K.-Y. Choi, and P. Lemmens, Weak first-order quantum phase transition in the spin-tetrahedron system $Cu_2Te_2O_5Br_2$ without lattice contributions, Phys. Rev. B **83**, 134403 (2011).

[41] E. G. Sergeicheva, S. S. Sosin, L. A. Prozorova, G. D. Gu, and I. A. Zaliznyak, Unusual magnetic excitations in the weakly ordered spin-$\frac{1}{2}$ chain antiferromagnet Sr_2CuO_3: Possible evidence for Goldstone magnon coupled with the amplitude mode, Phys. Rev. B **95**, 020411(R) (2017).